Assessing volcanic hazard and exposure in a data poor context: Case study for Ethiopia, Kenya, and Cabo Verde

S.F. Jenkins [a,*], K. Mee [b], S.L. Engwell [c], S.C. Loughlin [c], B.V.E. Faria [d], G. Yirgu [e], Y. Bekele [f], E. Lewi [g], C. Vye-Brown [c], S.A. Fraser [h], S.J. Day [i], R.M. Lark [b,j], C. Huyck [k], J. Crummy [c]

[a] Earth Observatory of Singapore, Asian School of the Environment, Nanyang Technological University, Singapore
[b] British Geological Survey, Environmental Science Centre, Keyworth, Nottingham, United Kingdom
[c] British Geological Survey, The Lyell Centre, Edinburgh, UK
[d] Instituto Nacional de Meteorologia e Geofísica, Mindelo, Cape Verde
[e] School of Earth Sciences, Addis Ababa University, Addis Ababa, Ethiopia
[f] Geo-hazard Investigation Directorate, Geological Survey of Ethiopia, Addis Ababa, Ethiopia
[g] Institute of Geophysics, Space Science and Astronomy, Addis Ababa University, Addis Ababa, Ethiopia
[h] Fraser Disaster Risk Consulting Ltd, Brighton, United Kingdom
[i] Institute for Risk and Disaster Reduction, University College London, United Kingdom
[j] School of Biosciences, University of Nottingham, United Kingdom
[k] ImageCat Inc, Long Beach, California, USA

ARTICLE INFO

ABSTRACT

Volcanoes produce a wide variety of hazards across varying spatial and temporal scales. When data are scarce on past eruptions and hazards, it can falsely imply low hazard recurrence and create challenges for robust hazard and risk assessment. Data quality and quantity vary considerably across different regions, volcanoes, and eruptions. Yet, there is a need for regional to global scale information on volcanic hazard and risk, where consistent and reproducible methods are applied. Such information is used by international stakeholders to inform funding priorities, risk reduction policies, and to highlight data and knowledge gaps, contributing towards the Sendai Framework's Sustainable Development Goals. Challenges in gathering this information can be most problematic where large populations are exposed to potential volcanic hazards but there are few comprehensive eruptive histories, as in sub-Saharan Africa. Here, we present a unique study to evaluate hazard and exposure for nine volcanoes in Ethiopia, Kenya and Cabo Verde, as part of an international project to develop multi-hazard Disaster Risk Country Profiles. We applied a two-stage expert elicitation process to volcanoes for the first time, and coupled the results with vent mapping, numerical hazard modelling, and GIS analysis of eight exposure categories to identify where high volcanic hazard and exposure coincide. Testing the sensitivity of our findings to input assumptions, to better understand where uncertainties lay, showed that improving our knowledge of past eruption volumes, frequencies, and dates was key to reducing uncertainty. Expert elicitations proposed that Fogo, Cabo Verde, is the most likely to erupt (eruption on average every 25 years), while Fentale (Ethiopia), Longonot and Suswa (Kenya) were elicited to have the greatest probability for a large explosive (VEI $\geq$ 4) eruption (on average every 400 years). Menengai and Longonot produce the larger exposure values across most VEI scenarios and categories of exposure, but population and GDP exposure was also large for more distal tephra fall and flows at Corbetti and Suswa, with order of magnitude increases expected between 2010 estimates and 2050 projections. Potentially high impact scenarios include tephra being dispersed across large cities (e.g. Nairobi, 55 km from Suswa) and key infrastructure (e.g. geothermal power station ~2.5 km from Aluto), as well as important tourist destinations, seats of government and emergency management operations (e.g. islands east of Fogo). This study provided the first hazard and exposure assessment of its kind for these volcanoes and drew attention to volcanic risk at the levels required to inform policy and future in-country funding opportunities.

* Corresponding author.
  E-mail address: susanna.jenkins@ntu.edu.sg (S.F. Jenkins).

1. Introduction

There is a need for information on how, when, where, and to what extent a volcano threatens its surroundings across two distinct spatial scales: i) the local scale, used to inform volcanic risk management for a volcano or population settlement/s and infrastructure. Local hazard and risk assessments should always be carried out within the context of the local physical, volcanological, and socio-cultural setting, and wherever possible led by, or at a minimum inclusive of, local scientists who are familiar with the volcano and have access to data on its past and current behaviour; and ii) at a regional to global scale, where multiple volcanoes and countries may be considered; this is used to inform broader policy or government advice. At a regional to global scale, consistency in the approach and treatment of available data is key in ensuring that hazard and risk calculations are repeatable and comparable. The primary purpose of regional to global scale assessments is typically to identify locations where more detailed, local assessments need to be carried out. Where such detailed, local assessments are not then forthcoming owing to a lack of funding, time and/or local to regional technical and scientific capacities, more generalised regional to global scale assessments can still be useful for awareness-raising, planning, and policy purposes.

This paper is concerned with regional to global scale hazard and risk assessments, which are required by an increasing array of practitioners and decision-makers [1]. Such assessments are used to inform national, regional, or global disaster risk reduction policy (e.g. Government agencies, The World Bank Group, United Nations) and management (e.g. insurance industries). However, they are often financially and/or time restricted, and it is - often incorrectly - assumed that data are readily available for a fast application of tried and tested methodologies that generate volcanic risk products. For volcanoes, the opportunity to highlight volcanic threat at the levels required to inform policy and future funding opportunities for in-country scientists is invaluable, but the difficulties in creating and analysing new data, for example through field studies, makes such regional or global studies challenging. From a disaster risk reduction perspective, capturing the many and multi-faceted hazards and impacts produced by volcanoes, and presenting one coherent view of the 'risk', is very challenging so outputs are driven strongly by stakeholder needs and data availability.

This paper describes a quantitative approach to regional hazard and exposure assessment for nine data-poor volcanoes in Ethiopia, Kenya and Cabo Verde, where there was minimal possibility to collect or analyse new data. The work represented the first volcanic hazard and exposure assessment of its kind for these volcanoes, producing data and findings that informed regional multi-hazard risk profiles. We developed a new framework for assessing hazard and exposure at volcanoes with few data, by creating data where possible and linking a sequence of established models. A two-stage expert elicitation process was applied to volcanoes for the first time to fill in key data gaps, address uncertainties, and to incorporate knowledge from those familiar with the volcanoes and region. Vent mapping and numerical hazard modelling was then used to refine the spatial distribution of likely future hazards before exposure was calculated. In what follows, we provide background on the unique context of the project and the case study area, before outlining our methodological approach (Section 2), results, and the sensitivity of outputs to the underlying assumptions (Section 3). We then discuss the knowledge gaps that need to be filled in order to move regional to global scale assessments forward (Section 4), before concluding.

1.1. Project context

This study contributed to multi-hazard Disaster Risk Country Profiles commissioned by the Global Facility for Disaster Reduction and Recovery (GFDRR) as part of the ACP-EU funded Africa Disaster Risk Financing Initiative (published here https://www.gfdrr.org/en/disaster-risk-profiles). The initiative was launched in 2015 and implemented by GFDRR and the World Bank alongside several partners,

including the African Development Bank, African Union Commission and the United Nations International Strategy for Disaster Risk Reduction. The Africa Disaster Risk Financing initiative included volcanoes in Disaster Risk Country Profiling for the first time, and aimed to support the development of risk financing strategies at the regional, national and local level in order to catalyse dialogue with governments in the sub-Saharan African region. Several hazards were included in the initiative: floods & droughts; earthquakes; volcanic eruptions; and landslides. Under the umbrella of the 'Global Volcano Model', an international network that aimed to create information on volcanic hazard and risk (www.gtr.ukri.org/projects?ref=NE%2FI030038%2F1), we responded to the call to assess hazard and exposure for volcanoes. We undertook this work to demonstrate that, while there is a significant challenge in terms of availability and accessibility of volcanic data, outputs that are useful to local through international stakeholders can still be achieved if we draw on the experience of the local and international scientific community.

1.2. Case-study area

Despite large numbers of very visible active volcanoes in sub-Saharan Africa, historical and geological data about eruptions in this region are more limited than any other volcanic area in the world: as a region, Africa has the highest proportion of undated Holocene volcanoes ([2]; Yirgu et al., 2014). We focussed our approach on three sub-Saharan countries identified by GFDRR for volcanic analyses - Ethiopia, Kenya, and Cabo Verde. The volcanoes lie in two distinct tectonic settings: the East African Rift (Ethiopia and Kenya) and a hotspot (Cabo Verde) (Fig. 1). The spreading apart of the African, Arabian and Somalian plates to form new crust in the East African Rift results in a dense concentration of large volcanic complexes that produce both rhyolitic and basaltic eruptions, basaltic monogenetic small cones and low-lying rift volcanoes that orientate along multiple elongate fissures [3,4,5] (Fig. 1a). The volcanoes of Cabo Verde lie above a hotspot with near-stationary relative movement leading to long (multi-million year) volcanic lifetimes for each island [6], with volcano typologies indicative of past large explosive eruptions as well as small-scale monogenetic volcanism (Fig. 1b). Many of the volcanoes across both the East African Rift and Cabo Verde exhibit both effusive and explosive eruption styles over time.

Of 118 Holocene volcanoes in the Smithsonian Institution's Global Volcanism Program defined region of Africa and Cabo Verde, 62% ($n = 73$) lie within the three countries defined for this study (50 in Ethiopia, 21 in Kenya and 2 in Cabo Verde). We deliberately did not consider all volcanoes across Ethiopia, Kenya and Cabo Verde, but focussed on target volcanoes. The project focussed analysis on large, central volcanoes with the potential to produce explosive eruptions with significant impact. For identifying appropriate target volcanoes in the study countries, we prioritised volcanoes with high population exposure [7] and took advice from local partners and colleagues familiar with the East African Rift and Cabo Verde volcanism to constrain the choice further based on hazard assessment needs and data availability. Corbetti, Aluto and Fentale volcanoes in Ethiopia, Menengai, Longonot and Suswa in Kenya and Fogo, Brava and Santo Antão in Cabo Verde were chosen (Fig. 1; volcano information in Supplementary Material A).

Historical data on volcanic activity and impacts across the target volcanoes (and countries) are limited, reflecting a broad knowledge gap; most historically dated eruptions occur only after the opening of the Suez Canal in 1869 (Ethiopia and Kenya) and the arrival of Portuguese settlers in 1460 (Cabo Verde), with detailed records for Cabo Verde only available from 1755 (following the loss of records in the 1755 Lisbon earthquake and fire). Should the eruption record be considered complete, the effect of the under-recording would likely be an under-estimation of the hazard posed by these volcanoes [2], especially in relation to the lower-frequency, higher-intensity and hazard volcanic events. Projects such as RIFTVOLC (2014–2021) were initiated on the basis of the limited data and have recently worked to fill some of these
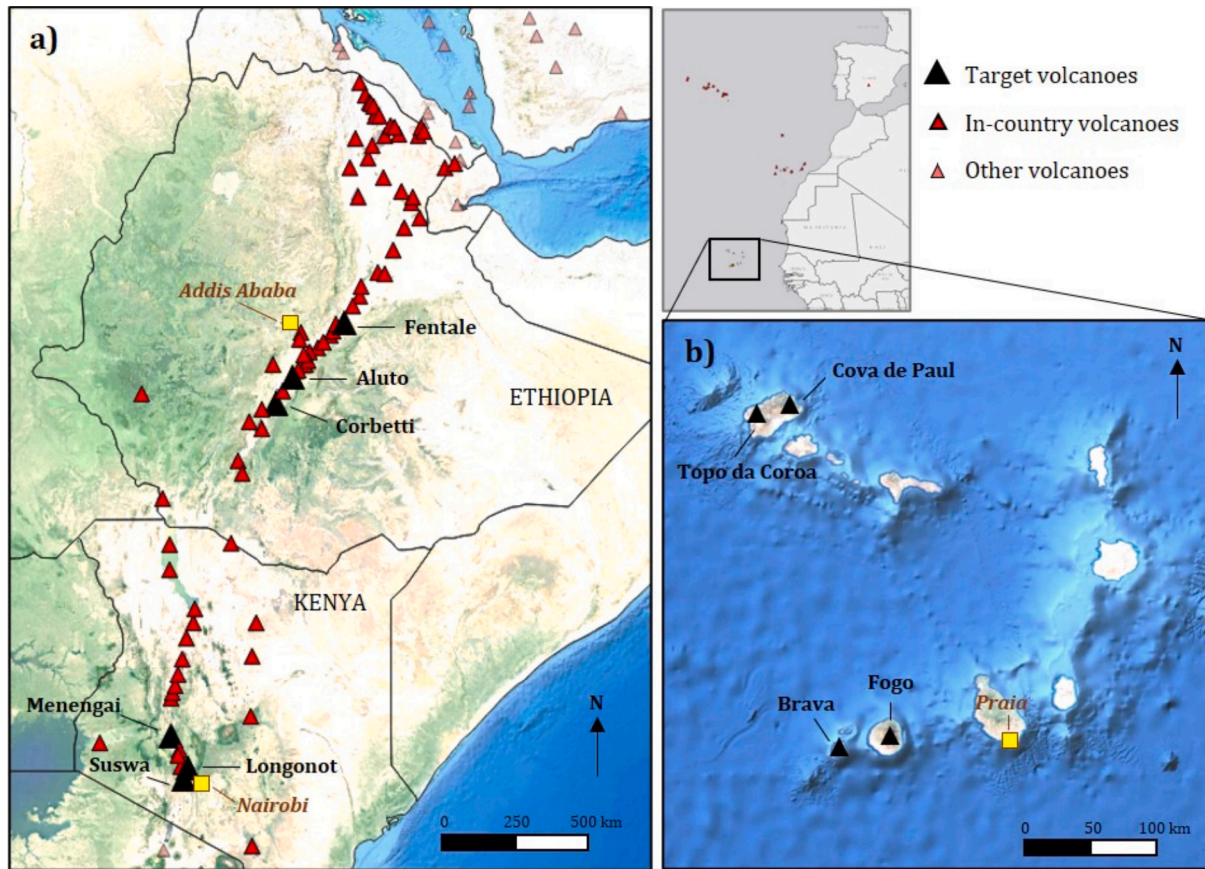
Fig. 1. The distribution of Holocene active volcanoes and the target volcanoes considered in this study in a) Ethiopia and Kenya, and b) Cabo Verde, with the location of Cabo Verde off the west coast of Africa shown in the small inset. Capital cities are shown as yellow squares. (For interpretation of the references to colour in this figure legend, the reader is referred to the web version of this article.)
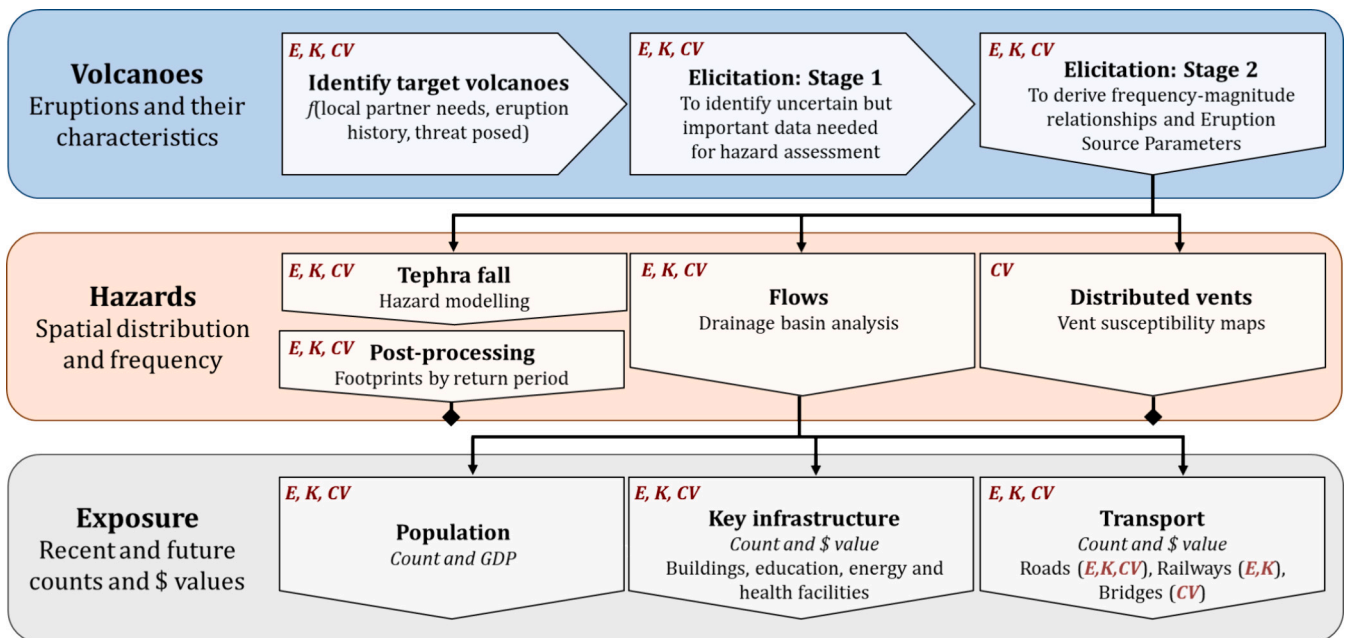

Fig. 2. Schematic of the components of our study. The countries for which each component was applied are shown in dark red italics: Ethiopia (E), Kenya (K) and Cabo Verde (CV). Black diamonds represent repeated nodes, i.e. the same exposure analysis was applied to tephra fall and volcanic field hazards as for flows. (For interpretation of the references to colour in this figure legend, the reader is referred to the web version of this article.)

knowledge gaps to support hazard assessment (e.g. [8,9,10,11,12]; [13]; [14,15,16]), but many of these studies post-dated development of the GFDRR Disaster Risk Country Profiles.

2. Approach

There were three main components to our approach (Fig. 2): 1) A two-stage expert elicitation to define appropriate volcano and eruption analogues, frequency-magnitude relationships and to discuss potential crisis scenarios; 2) Hazard quantification through numerical modelling and geospatial analysis; 3) Exposure assessment by coupling hazard layers with data on recent and future projections of population and infrastructure.

2.1. Expert elicitation

The lack of data available for any of our target volcanoes required an 'expert judgement' approach. The purpose of the elicitations was to formalise our understanding, best estimates and uncertainty in the characteristics and frequencies of explosive events at volcanoes in Ethiopia and Kenya and, in a separate elicitation, Cabo Verde. There were two stages to the elicitation:

1. *'Sanity check' questionnaire* (Supplementary Material B), carried out by email to allow for the inclusion of a greater number of in-country scientists who were not able to attend the formal elicitation. The results were used to identify where the greatest uncertainties lay and to focus discussion.
2. *Formal elicitation* (Supplementary Material C), conducted over a 1.5 day in-person workshop for Ethiopia and Kenya and a 0.5-day teleconference workshop for Cabo Verde. The elicitations were used to formally elicit frequency-magnitude relationships for each of the selected volcanoes, as well as to refine likely Eruption Source Parameters (ESPs). Importantly, the elicitation allowed the uncertainty associated with our estimates to be quantified.

Participants invited to join the expert elicitation were selected based on their knowledge of volcanism in the target settings and experience of analogous settings. All participants received the same background documentation, distributed prior to the elicitation with feedback invited. The participants in our panel knew each other's experience and expertise, and the elicitation was co-facilitated by a statistician with experience of the process (author RML) and a volcanologist (author SFJ). Facilitation ensured that dominant personalities did not monopolise the discussion.

The second 'formal' stage of the elicitation used the SHeffield ELicitation Framework (SHELF) and software (Oakley and O'hagan, 2010), where to the best of our knowledge it was applied to volcano data for the first time. Formal elicitation aggregates the elicited opinions of a panel of experts into a single outcome. A common approach to this [17] weights each panellist based on their performance addressing test or "seed" questions. This requires a substantial number of known cases for the seeding process (at least 10, and probably more; Clemen, 2008). For our target volcanoes, this would be particularly challenging; the lack of data is the primary reason for considering elicitation. We therefore chose to instead apply the SHELF framework for group elicitation, which uses behavioural aggregation to work towards a consensus view from a panel. In behavioural elicitation, the group forms individual views on the target distribution, then holds a facilitated discussion with the aim of arriving at a consensus view. This process uses feedback, which allows the participants to visualise the effects of proposed changes to the elicited distribution on its shape and the value of selected quantiles. Behavioural aggregation was favoured here because of its transparency, and suitability for ensuring that members with varied experience were able to contribute to the formation of a consensus view based on explicit technical argument from limited data, considerable uncertainty and the

risk that individual participants, of varied statistical facility and knowledge, might not all interpret the questions consistently in individual consideration. For more information on the SHELF elicitation framework, the reader is directed to Gosling [18].

2.2. Hazard modelling

The spatial distribution, intensity and frequency of hazard was assessed for three volcanic processes (Fig. 2), to address the wide spatial hazard of tephra fall, the more proximal but deadly hazard from volcanic particle flows (pyroclastic density current and lahar), and the spatial variability for new eruptive vents in Cabo Verde. The following subsections describe our modelling approach for each of the three hazard quantification components.

2.2.1. Tephra fall

The distance and area over which tephra is dispersed is strongly controlled by wind direction and speed, which varies with distance from the vent and with altitude above the vent, affecting particles as they fall through the atmosphere. While wind conditions have a strong control, tephra dispersal is also affected by the size, shape and density (and therefore fall velocities) of the particles, and the eruption style, intensity and magnitude. In considering the potential hazard from tephra fall at our target volcanoes, we employed the numerical model Tephra2 [19], which can account for the complexities in reproducing ash dispersion and deposition while being simplified enough to permit modelling of a large number of potential explosive events and wind conditions. The required output for each of the target volcanoes, was a footprint (spatial representation) of tephra thickness at a given set of average recurrence intervals (ARI). The steps towards achieving this were:

1. Eruption frequency estimates for Volcanic Explosivity Index (VEI) 3 through 6 were defined for six central volcanoes in Ethiopia and Kenya and VEI 3 through 5 for the three central volcanoes in Cabo Verde through expert elicitation;
2. Seasonal wind analysis of six-hourly ERA-Interim reanalysis data between 2006 and 2015 (0.75° resolution) was carried out for each volcano to give a preliminary indication of likely tephra dispersion during an explosive event (wind speed and direction with altitude) and after as a result of remobilisation (surface wind speed and rainfall);
3. For each of the volcanoes, Eruption Source Parameter (ESP) probability distributions were defined through expert elicitation;
4. Multiple VEI scenarios were simulated to span the range of potential explosive events at the volcano, with each VEI scenario simulated into 5000 different wind conditions, leading to 20,000 simulations for each volcano in Ethiopia and Kenya and 15,000 for each volcano in Cabo Verde;
5. A probabilistic model framework was developed to post-process the tephra thickness footprints and aggregate them to provide tephra thickness values at specific return periods (as described below).

The study mandated that all hazards (not just volcanic) provide intensity metrics as a function of at least three ARIs: 250, 500, and 1000 years to capture the lower-frequency, higher-consequence events that affect risk management decisions and to allow comparisons across hazards at consistent ARIs. This required that each simulation be assigned an annual simulation probability: the annual eruption probability for that VEI scenario (determined through expert elicitation) divided by the number of simulations run for that scenario (i.e. each simulated wind condition was considered equally likely). Post-processing of the individual tephra fall footprints to provide tephra loads for each ARI was achieved by ordering the simulated tephra fall loads from largest to smallest for each grid cell, and cumulating the annual simulation probabilities simulation-by-simulation until the inverse of the cumulated value was equivalent to the required ARI. The

corresponding simulation tephra fall load at that grid cell represented the hazard intensity that would be equalled or exceeded within the average recurrence interval being considered (following the method of [20]). Interpolation between simulations was sometimes required.

2.2.2. Flows

We chose to identify hazardous zones for gravity-controlled flows using a drainage basin analysis implemented in GIS (for step-by-step method see Supplementary Material E). Volcano locations were taken from the Smithsonian Institution's Global Volcanism Program (GVP), and generally assigned to either the highest point of the volcano or the youngest cone. The analysis used GIS tools applied to the freely-available SRTM digital elevation model to identify flow directions for each 30 m pixel within radii buffers, applied to the GVP-defined vent location, of 3 km (Cabo Verde, the extent being limited by small island setting) and 30 km (Ethiopia, Kenya) to suggest potentially hazardous areas for pyroclastic density currents, and 10 km (Cabo Verde) and 100 km (Ethiopia, Kenya) for lahars (following [21]). These flow directions allowed drainage basins that lay within the radii to be identified, with those draining from the volcano assumed to be more hazardous. The drawback to applying a hydrological analysis such as this is that it does not account for any physical characteristics of the flows and is in effect a gravitational inundation approach controlled by assumed maximum runout distances of volcanic flows. However, the reliability and accuracy of flow models requires more data than are currently openly available, e.g. a high-resolution DEM, the volume and runout of previous flows, the frictional resistance of the substrate.

2.2.3. Distributed vents

Spatial hazard assessment becomes complicated when the future vent location is not known. Volcanic activity across the three study islands in Cabo Verde has resulted in the formation of many flank vents. To tackle this, we estimated the probability of vent opening on each island by assuming a spatial correlation between past and future vent location (i.e. a new vent is more likely to form in locations where there is a high density of past vents). Identifiable previous eruptive vents (Holocene-Pleistocene) were mapped from satellite imagery and any missing were further identified by experts with on-island field experience. The spatial density of the resulting vents was modelled using Gaussian kernel density estimation (following [22]) to indicate areas with higher probability of vent opening. The kernel bandwidth was objectively defined using the SAMSE (Summed Asymptotic Mean Squared Error) bandwidth estimator, which in turn used an asymptotic mean integrated square error (AMISE) method [22]. This approach was chosen because it does not require information other than the location of past events and makes the simplest assumptions regarding the relation of past and future vents.

2.3. Exposure assessment

To assess exposure to the estimated volcanic hazard, we used GIS to combine our hazard footprints with population, GDP, the distribution and US dollar value of buildings, education, health and energy facilities, roads and railways. Data were provided to GFDRR by the risk management company ImageCat as part of the risk profiles project and applied also to the other hazards assessed for the multi-hazard risk profile. The data were derived from national, regional, and global mapped datasets from between 2010 and 2015, supplemented with manual and country/volcano-specific mapping efforts using Google Earth or other available imagery where possible, and were provided at a 30 arc-second (~1 km) resolution. Population and GDP values were also projected to 2050 (see Supplementary Material G.

For tephra fall, where impacts are gradational as a function of hazard intensity, we used three different loading thresholds: 0.5 kg/m^2, 10 kg/m^2 and 100 kg/m^2, approximately equivalent to thickness in mm, i.e. 0.5 mm, 10 mm and 100 mm given a dry tephra density of 1000 kg/m^2.

These thresholds were chosen to reflect the variable hazard posed by tephra falls (following [23]) of different thickness to enable the exposure of different types of infrastructure. For example, 0.5 mm of tephra fall is expected to have little impact on buildings, but can obscure road markings, as well as reduce traction and visibility, with implications for respiratory health in vulnerable individuals when resuspended. 10 mm of tephra is associated with minor damage to buildings and infrastructure, with significant clean-up required [24]. 50 mm of tephra can cause major agricultural productivity loss, with the potential of roof collapse for very weak buildings. For flows, we used the drainage basins to evaluate exposure.

For each hazard and hazard threshold, sixteen categories of exposure were estimated for each volcano and return period, giving >1200 distinct exposure estimates for tephra fall and >850 estimates for particulate flows.

3. Results

3.1. Expert elicitation

Responses to the initial questionnaire (Stage 1: Fig. 2; Supplementary Material B) showed that the greatest uncertainties lay in our estimates of frequency-magnitude at each of the volcanoes. Therefore, this is where we chose to focus formal elicitation efforts (Stage 2: Fig. 2; Supplementary Material C). Rather than elicit individually for each of the six selected volcanoes in Ethiopia and Kenya, the group felt that considering some volcanoes as analogues of each other (i.e. with properties similar enough to be considered exchangeable) would be more appropriate given the lack of data. Knowledge of the volcanic setting and magmatic composition, as well as the morphology of the volcanoes, was thus used to divide the volcanoes into three analogue groups:

- Aluto and Corbetti were considered viable analogues (both have had caldera-forming eruptions). Aluto was the better studied of the two and further information could be drawn from better-studied peralkaline systems such as Pantelleria (Italy), Mayor Island (New Zealand) and Gran Canaria (Spain).
- Menengai is quite distinct morphologically and appeared to have a higher frequency of explosive eruptions than Aluto or Corbetti; it was thus considered separately to the other volcanoes.
- Fentale, Longonot and Suswa had little to no information but were thought to be more frequently explosive than Aluto and Corbetti. Unlike Menengai, they are all characterised by a relatively recent summit caldera and approximately similar eruption histories. They bear similarities to Rungwe in Tanzania, which, as one of the best-known volcanoes in Africa, was considered an analogue here.

For Cabo Verde, there were no close global or regional analogues for any of the volcanic islands. Given the lack of recorded eruption history for Brava and Santo Antão, it was agreed that the formal elicitation could only reliably be attempted for Fogo volcano, where the most studies have been carried out and for which there is a historic eruption record.

Frequency-magnitude relationships, and their interquartile (25th to 75th) confidence bounds, were elicited (see Supplementary Material C for questions) separately for the three different volcano groupings and for Fogo (Fig. 3 and Table 1). The SHELF procedure is not forced to form a consensus view; however, a consensus was reached in all cases in this study.

The first stage of our elicitation provided feedback on our preliminary ESPs, which were mostly based on analogue volcanoes and existing methodologies for assessing tephra hazard at the large scale (e. g. [20,25,26]). Group discussions as part of the second stage were then used to agree upon reasonable parameter distributions and bounds, as
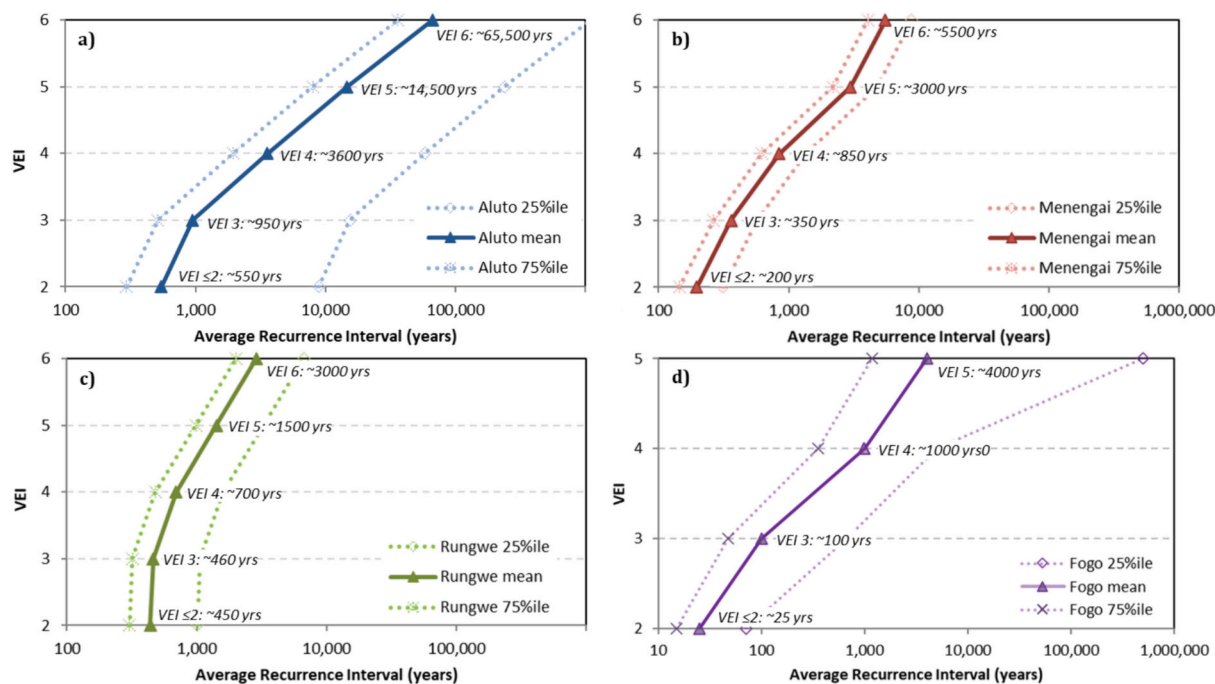
Fig. 3. Elicited frequency-magnitude relationships for a) Aluto and Corbetti, b) Menengai, c) Rungwe, which acted as an analogue for Fentale, Longonot and Suswa, and d) Fogo volcanoes. Note that Fogo shows probabilities for VEI ≤ 2 through 5, while all others extend to VEI 6. Solid lines represent the mean estimate and dashed lines the interquartile confidence bounds. The 75th percentile in probability gives the shorter average recurrence intervals, i.e. 75th percentile bounds lie to the left of the mean, 25th percentile to the right.

Table 1
Elicited average recurrence intervals (mean, with 25th to 75th percentile range in brackets) for each of the four volcanoes and for any VEI and each of the VEI classes considered in the elicitation.

	Average recurrence interval in years (25th – 75th percentile uncertainty range)					
	Any VEI	VEI ≤ 2	VEI 3	VEI 4	VEI 5	VEI 6
Aluto, Corbetti	308 (75–5000)	545 (295–8850)	950 (515–15,500)	3600 (1950–58,000)	14,500 (7950–250,000)	66,500 (36,000–1.08 Myrs)
Fentale, Longonot, Suswa (analogue: Rungwe)	144 (100–335)	440 (200–1000)	460 (320–1050)	690 (480–1600)	1400 (990–3300)	2850 (2000–6650)
Menengai	105 (75–165)	200 (145–315)	360 (265–575)	845 (620–1350)	3000 (2200–4750)	5550 (4050–8800)
Fogo	20 (10–65)	25 (15–70)	100 (50–665)	1000 (355–5000)	4000 (1200–500,000)	n/a

described in Supplementary Material D. In absence of data or information to justify otherwise, ESPs were considered to apply to all target volcanoes.

Volcanic eruptions are not discrete events, although they are often modelled as such, and so we also used the elicitation to glean information on likely eruption duration. For Ethiopia and Kenya, two durations of interest were considered: the explosive tephra-producing component of the eruption and the overall eruption duration. Despite limited observations available for historical eruptions in Ethiopia and Kenya, both explosive eruptions from Dubbi in 1861 [27] and Nabro in 2011 [28] exhibited a day or so of paroxysmal explosive activity that was followed by a few days of smaller tephra, gas and steam emissions and then approximately six months of effusive activity and gas emissions. The group concluded that for the purposes of modelling, eight hours of tephra-producing activity (following estimates for silicic eruptions from [29]) would be consistent with a waxing and waning plume over one day. For emergency management purposes, a good preliminary estimate of eruption chronology, for the target volcanoes in Ethiopia and Kenya, is that the paroxysmal explosive stage will be followed by smaller tephra and gas emissions over about one week and approximately six to twelve months of effusive activity. It was not possible to assign likely eruption durations to a future eruption on either Brava or Santo Antão in Cabo Verde, given the absence of historically-recorded eruptions on both

islands. However, geological studies show multiple deposits within the one eruption at both volcanoes, suggesting that eruptions may produce multiple stages of varying intensity and style over a drawn-out period. For Fogo, historical post-1725 eruptions indicate that eruptions continued for between 1 and 3 months; however, historical effusive eruptions prior to this may have been longer, continuing over a period of years. Thus, emergency management planning should consider months'- to years'-long eruptions.

3.2. Hazard modelling

3.2.1. Tephra fall

Winds across the study regions blow predominantly towards the east or west, following equatorial trade winds, with wind speeds increasing around the tropopause and with altitude above sea level. Their provenance and strength depend upon the season (Fig. 4). Wind speeds of 2 m/s are enough to remobilise irregular dry tephra particles (Fowler and Lopushinsky, 1986) suggesting that all of the study areas are susceptible to tephra resuspension (Fig. 5), which can cause repeated impacts over a wider area. Wind speeds are highest and rainfall amounts lowest, supporting tephra resuspension, for volcanoes in Cabo Verde; however, the relatively small island areas may act to limit the amount of tephra fall available for resuspension.
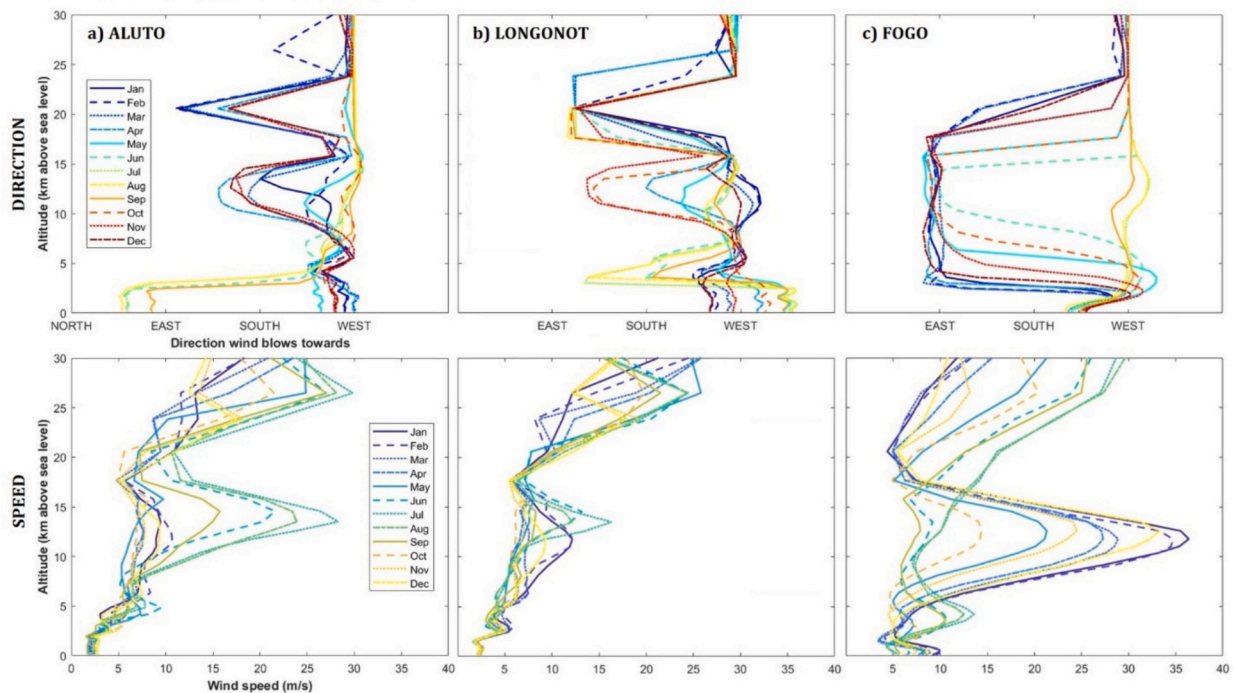
Fig. 4. Wind directions (upper) and speeds (lower) with altitude for the wind record closest to a) Aluto (and indicative for Corbetti and Fentale), b) Longonot (indicative for Menengai and Suswa), and c) Fogo (indicative for Brava and Santo Antão). Ten years (2006–2015) of ECMWF ERA-Interim reanalysis records at 6 hourly interval records provide the base data, with median data shown for each month. The rainy season/s in central Ethiopia (Aluto) being March to May and June to September, in Kenya (Longonot) being March to June and November to January, and in Cabo Verde (Fogo) being July to October.

For all volcanoes, the east-west dominant wind directions elongate the tephra fall footprint meaning that areas to the north or south of a volcano are less likely to be affected by tephra, although single simulations highlight that it is possible and can as a result affect large population centres (Fig. 6 lower). Tephra falls in Ethiopia and Kenya are expected to impact communities to the west of the volcanoes more frequently because of the predominantly easterly winds in the region at altitude (Fig. 6; Supplementary Material D). The faster attenuation in tephra thicknesses at the larger return periods (500 and 1000 years), Menengai, Fentale, Longonot, and Suswa, relative to Fogo, are the result of higher elicited VEI $\geq$4 probabilities (Fig. 6), meaning that the impacts associated with large tephra thicknesses would be expected more frequently and over a wider area around mainland case study volcanoes than at Fogo.

In modelling tephra fall hazard, we used expert-derived ESPs. To test the influence that these ESPs had on our outputs, we carried out one-at-a-time sensitivity testing – where inputs were varied between the minimum and maximum of the simulated range – for a VEI 5 scenario from Corbetti. As ESPs (except wind conditions) are consistent across volcanoes and tephra loads scale linearly with erupted mass in Tephra2, sensitivity testing results were applicable across all volcanoes. Sensitivity testing showed (Fig. 7) that:

1. Overall, the largest source of uncertainty was the erupted mass;
2. Total grain size distribution was important, with the choice of median grain size more influential than erupted mass on tephra thicknesses in proximal areas (<30 km);
3. When plume height increased or when particle density or median size decreased, there was a relative increase in tephra accumulation farther from the vent and relative decrease closer to the vent.
4. Changes to the diffusion coefficient or fall-time threshold showed negligible (< 1%) change in simulated tephra load in distal reaches (>100 km from the vent).

These findings are mostly in agreement with those of Scollo et al. [30], who similarly identified erupted mass as the ESP with the greatest influence on simulated thicknesses.

3.2.2. Flows

Potentially hazardous areas determined by the basin analysis are provided for all volcanoes in Supplementary Material E, and show that sharp topographic changes strongly control area and shape of the footprint (e.g. Fig. 8).

We tested the influence of assumed vent location and the resolution of the DEM on drainage basin analyses. While we used case study volcanoes to show sensitivities, the findings are applicable to all volcanoes. Fig. 9 exemplifies the large effect that vent location could have on the drainage basin analysis; it shows the effect of calculating drainage basins at Suswa and Fentale using two different vents located within the same summit caldera: one using the GVP location at the time of our study and the second using the centre of the crater, <3 km away and derived from the underlying DEM. Fig. 10 shows the influence of DEM resolution on drainage basin footprints in Cabo Verde, comparing the results using 450 m resolution (used by Aspinall et al. [21] and freely available 90 m and 30 m SRTM DEMs. Strong proximal topography like the ~1000 m high walls surrounding the collapse scar of Fogo acted to constrain the drainage basins that lie within 3 km of Pico do Fogo, but not 10 km. The inclusion of nearly the entire island of Brava for both 3 km and 10 km buffers at all resolutions (Fig. 10) suggests that the whole island is susceptible to flows, which is supported by the abundant island-wide PDC deposits found on Brava (Simon Day, pers. Comm.). A resolution of 450 m appeared too coarse to capture topography, whereas a resolution of 30 m or higher caused the drainage basin analysis to be overly influenced by local topography.

3.2.3. Distributed vents

Varying numbers of vents were identified through remote mapping using available satellite imagery for each of the three islands of Fogo (*n*
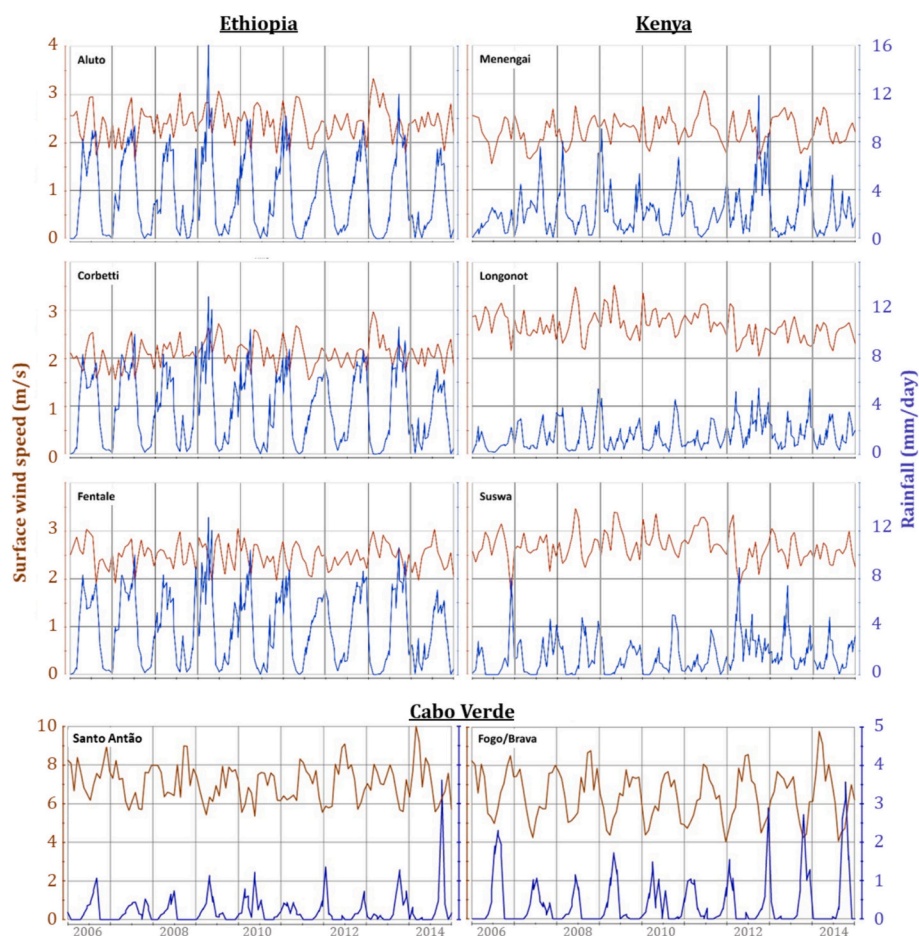
Fig. 5. Wind speed (brown line) and rainfall (blue line) for the period 2006 to 2015 at each of the volcanoes in our study, sourced from ECMWF ERA-Interim six-hourly reanalysis data. Note that Cabo Verde axes limits are different: wind speeds are higher and rainfall amounts lower than for the mainland Africa study areas. (For interpretation of the references to colour in this figure legend, the reader is referred to the web version of this article.)

= 115), Brava ($n = 29$) and Santo Antão ($n = 76$), which are provided alongside the vent spatial density maps in Supplementary Material F. For Brava, on-island vents include phreatomagmatic maars, lava domes and effusive vents of various morphologies and sizes, with effusive vents being very rare. Spatial density analysis identified a broad region of higher densities extending from the main town of Vila Nova Sintra in the north, which is built on the flat ground inside an old phreatomagmatic maar crater, through the centre of the island to the south (Fig. 11). As on Brava, in Santo Antão there are a large range of vent types and sizes, ranging from phonolite domes to phreatomagmatic maars. Analysis of the identified vents showed a clear bimodal distribution, with two areas of higher density, one to the east and one towards the west of the island (Fig. 11), coinciding with the two main volcanoes of Cova de Paul and Topo de Coroa. These represent the first spatial density maps for these two islands.

Preservation bias may affect the identification of vents on Fogo and Santo Antão due to the greater rates of erosion in the canyon systems to the north of the island. Also, in areas of more recent activity, burial of older vents may skew the vent susceptibility analysis to show higher relative probabilities in those areas where vents are better identified (i.e. where less recent activity has occurred). Consistent and reliable vent age data were not available for any island in Cabo Verde, but a 1680 tephra layer from Pico do Fogo, which blanketed the island, meant that we could distinguish post-1680 ($n = 57$) vents on Fogo. We ran two separate analyses to evaluate the effect of vent age on our results: i) with all available vent information, and ii) with the post-1680 vents only, (Fig. 12; Supplementary Material F).

Higher spatial densities on Fogo were elongated within a north-south zone of Chã das Caldeiras when considering only post-1680 vents, reflecting their clustering within Chã [31]. This clustering led to a reduced area of elevated probabilities for vent opening, with increased probability, compared to when pre- *and* post-1680 vents were considered. For all vents, higher densities extended outside of Chã to the north, south-east, and more broadly to the west. The north-northwest and the coastal areas, including the main town of São Filipe in the west, are, for the most part, low probability areas for new vent opening, regardless of the vent data used.

3.3. Exposure assessment

We plot a selection of exposure values in Fig. 13 for the target volcanoes of Ethiopia and Kenya; all exposure data are provided in Supplementary Material G. Exposure on the Cabo Verde islands is smaller relative to the mainland volcanoes of Ethiopia and Kenya because of the island setting (smaller land area) and lower population density. Areas of higher population density typically relate to areas with higher GDP and greater amounts of infrastructure, and so the presence of cities within our hazard footprints had strong effects on calculated and projected exposure. For example, the city of Nakuru (population ~ 0.5 M), 7.5 km south of Menengai and 75 km northwest of Longonot, causes the relatively large exposures for Menengai and Longonot across all categories, while the impingement of the 0.5 mm thickness threshold footprint on Nairobi (population ~ 5.5 M), 55 km to the east-southeast of Suswa, leads to a large increase in population and building values for this
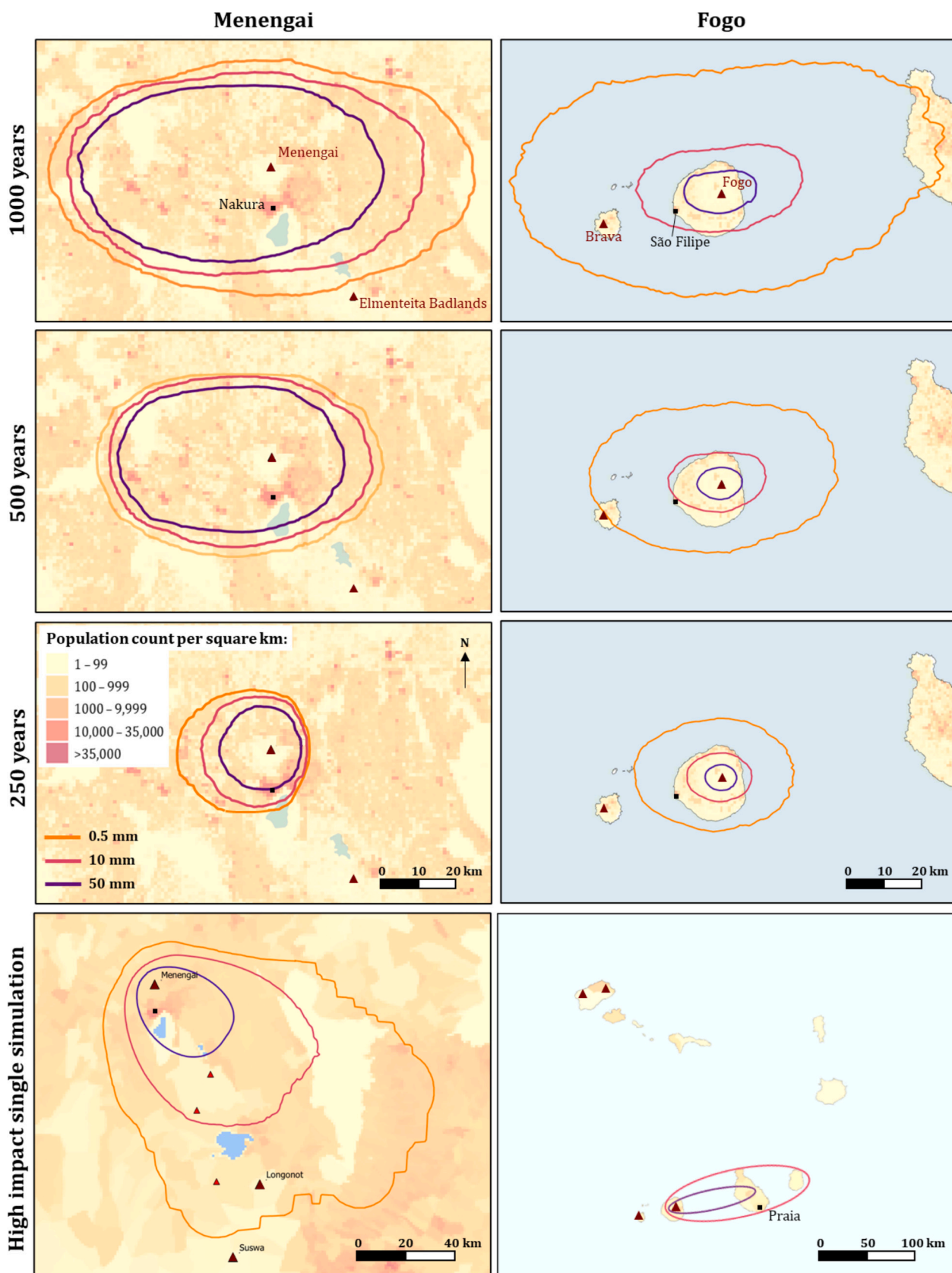
Fig. 6. Calculated tephra fall contours for the three thresholds used for assessing exposure: 0.5, 10 and 50 mm, for Menengai volcano in Kenya (left) and Fogo volcano in Cabo Verde (right) for the three return periods defined by GFDRR: 1000 years (upper), 500 years (upper middle), 250 years (lower middle), and for a VEI 4 simulation that impacts large population centres (lower). Underlying population density data from Landscan (2019).
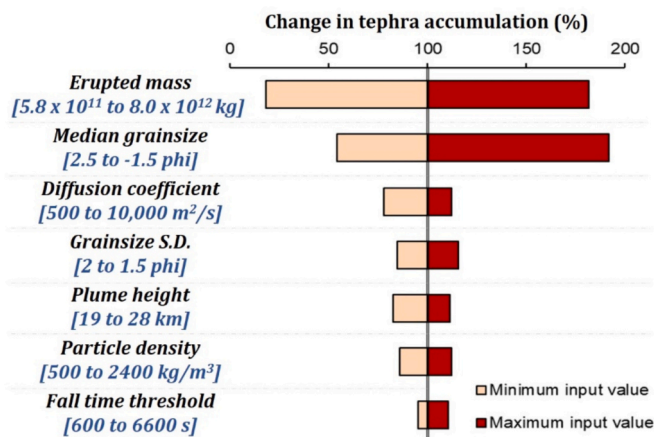
Fig. 7. Sensitivity analysis results for the downwind tephra accumulation of a VEI 5 eruption. Each input parameter was varied to credible minimum and maximum values [given by the values in brackets], with every other parameter fixed. The absolute change (as a %) in tephra accumulation averaged over a downwind transect at 5 km intervals is shown. The greater the range of change in tephra accumulation, the greater the influence on the outputs.

threshold. Projected GDPs in 2050 are large, typically around one order of magnitude larger than calculated for 2010, for all volcanoes, hazards and thresholds; for example, for the drainage basin analysis within 30 km of Corbetti's vent GDP increases from 259 million (2.59×10^8) US\$ in 2010 to 2.96 billion (2.96×10^9) US\$ projected for 2050 (Fig. 13).

Population exposure was identified as a potential source for uncertainty through discussions with local partners in Ethiopia and Kenya. Comparing populations using three different gridded population datasets (WorldPop, LandScan, GPW), showed that LandScan consistently results in smaller exposed populations than WorldPop or GPW (for example, ~1.17 million people versus 1.19 and 1.60 million, respectively within 30 km of Corbetti), but that relative differences in exposure

across the volcanoes was consistent within and across the datasets (Table 2), likely because similar underlying dysymentric mapping algorithms are applied.

4. Discussion

Fogo volcano in Cabo Verde was considered the volcano most likely of the four elicited volcanoes to erupt in the near future, with a relatively high probability of low VEI ($\leq$2) eruptions giving an average recurrence interval of ~25 years (Fig. 3d). Corbetti and Aluto were considered the least likely, with the probability of explosive eruption (VEI $\geq$ 3 eruption every ~700 years) aligning with those estimated from field mapping (~1000 years, Corbetti: [10]), tephra deposits in lake sediments (~900 years, Aluto: [35]) and event tree development [12], although our uncertainties were larger. For Aluto, our mean eruption frequency for any VEI aligns well with the maximum estimated from recent field studies (1 to 3 events per 1000 years: [14]). For all volcanoes, the elicited confidence in eruption frequencies decreased as the VEI increased, reflecting two different sources of uncertainty: i) deposit data; and ii) future behaviour of the volcano. For Fogo, our elicited values are lower and with wider uncertainty for VEI 5 eruptions (every ~4000 years) than in published literature (every ~2000 years: [36]) because elicited expert feedback allowed for the possibility that previously considered primary tephra layers were actually reworked deposits. For Aluto/Corbetti and Rungwe (elicited as an analogue for Fentale, Longonot and Suswa) volcanoes, larger uncertainties for VEI 5 and 6 eruptions reflected the potential for the system to move towards extinction or to experience the very long repose intervals that seem possible at peralkaline volcanic systems. The relatively small probability for VEI 5 and 6 eruptions reflected the small, but not zero, chance that the volcanoes revert back to caldera-forming activity of approximately 200 to 300,000 years ago [10]. Overall, the elicitation exercise highlighted the large uncertainties associated with estimating frequency-magnitude at data-poor volcanoes, particularly the larger intensity, lower frequency explosive eruptions, as recognised for other volcanoes [37,38]. This reinforced the importance of including these uncertainties when communicating
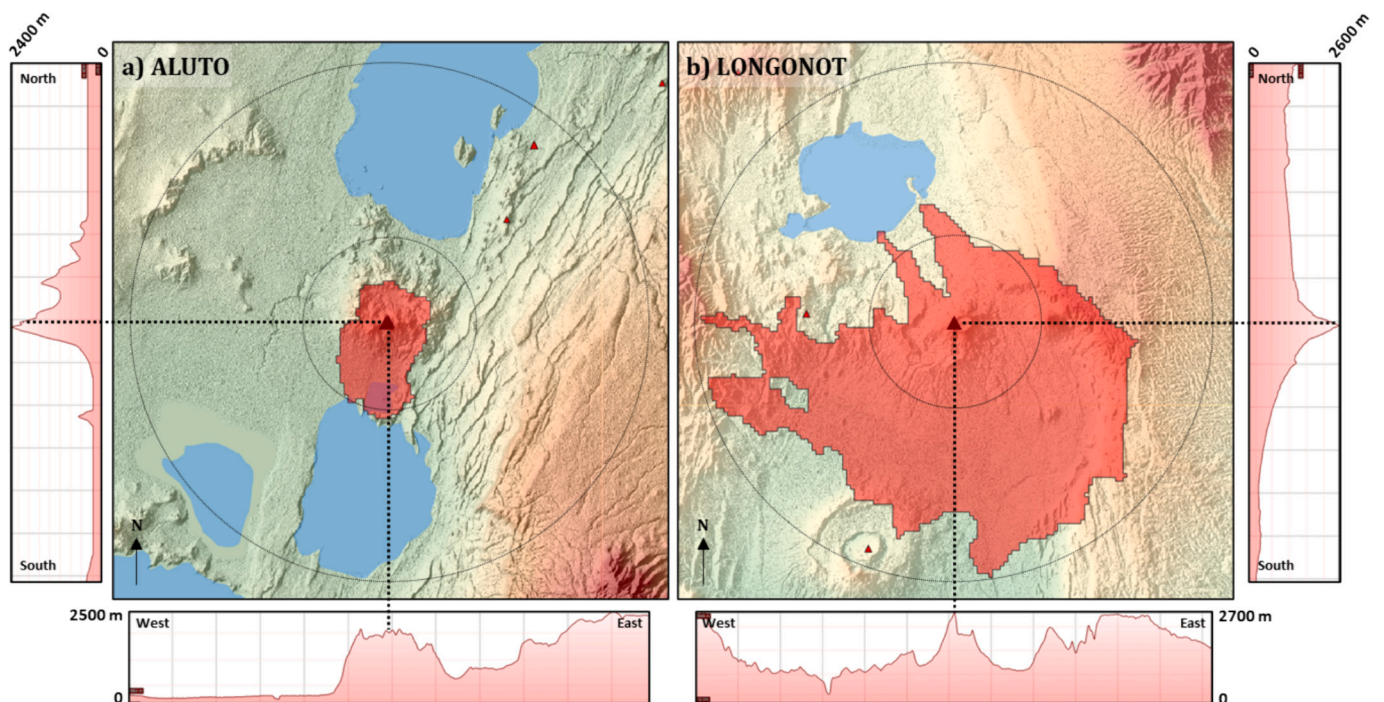

Fig. 8. Drainage basin analysis outputs using 30 km outer radii, indicative of PDC hazard, for a) Aluto volcano in Ethiopia, which shows the smallest footprint, and b) Longonot volcano in Kenya, which shows the largest footprint of our target volcanoes. North-South and West-East elevation profiles are shown for +\- 30 km either side of the GVP-defined vent; 10 x vertical exaggeration. Inner radii are 10 km, and simply for information.
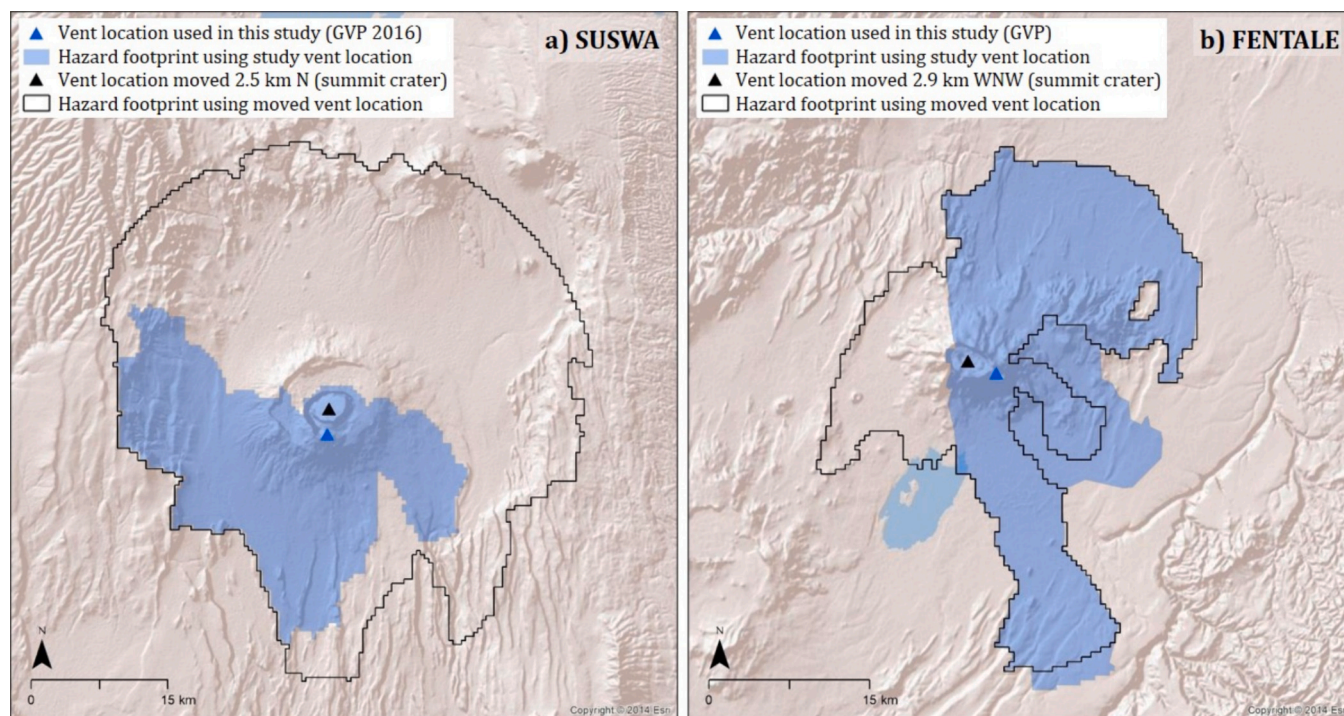
Fig. 9. Potential hazard zones produced by the drainage basin analysis for a 30 km buffer applied to: a) Suswa in Kenya and b) Fentale in Ethiopia when two different vent locations are used: that given by Smithsonian Institution's Global Volcanism Program at the time of our study (blue triangle and shaded area) and that given by the centre of the summit crater (black triangle and outline). (For interpretation of the references to colour in this figure legend, the reader is referred to the web version of this article.)
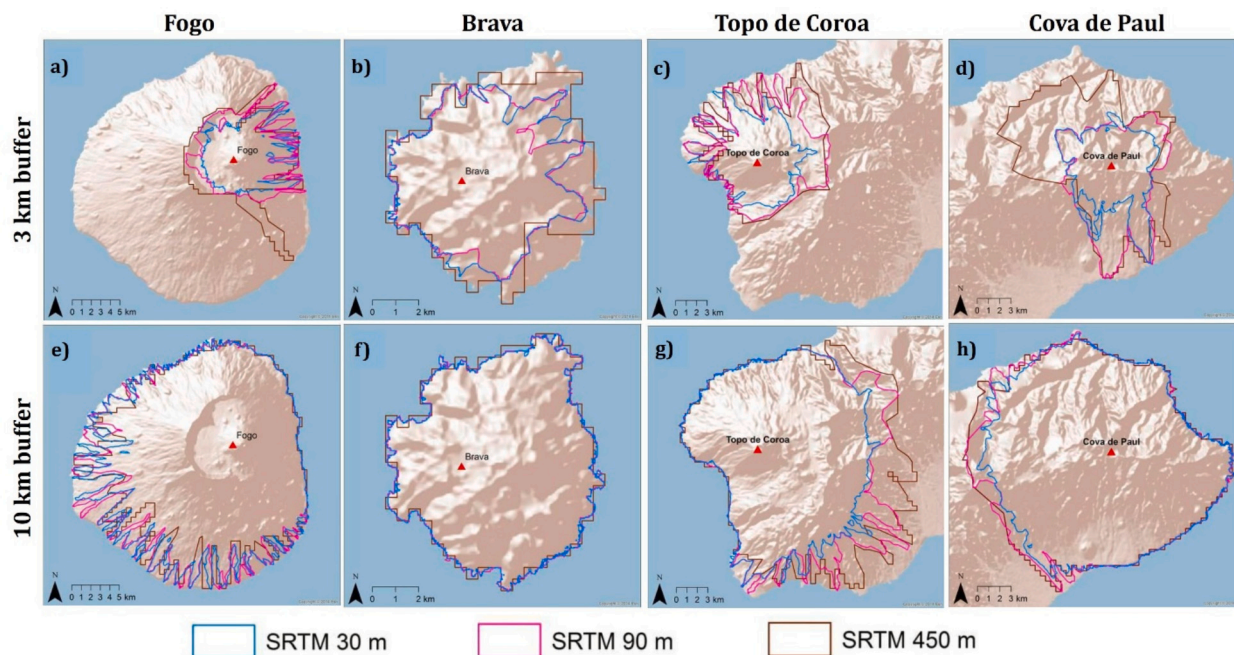

Fig. 10. Drainage basin analyses footprints created using two different buffer extents: 3 km (top) and 10 km (bottom) and from three different DEM resolutions for a/e) Fogo, b/f) Brava, c/g) Santo Antão – Topo de Coroa, d/h) Santo Antão – Cova de Paul.

eruption probability estimates.

Modelling tephra dispersion in this region for the first time highlighted the strong seasonal influence on the hazard for this region. For example, westerly winds during the dry and windy season (October through June) in Cabo Verde disperse tephra from the volcanic islands in the west across the other islands to the east. Simulations show that the

capital city of Praia, the official volcano monitoring agency (Instituto Nacional de Meteorologia e Geofísica: INMG) in São Vicente, and the two popular tourist destinations of Sal and Boa Vista would all be preferentially affected during the dry season (Fig. 6), with the potential for tephra remobilisation and repeated impacts. As the deposit thickness associated with a given return period provides an aggregated result and
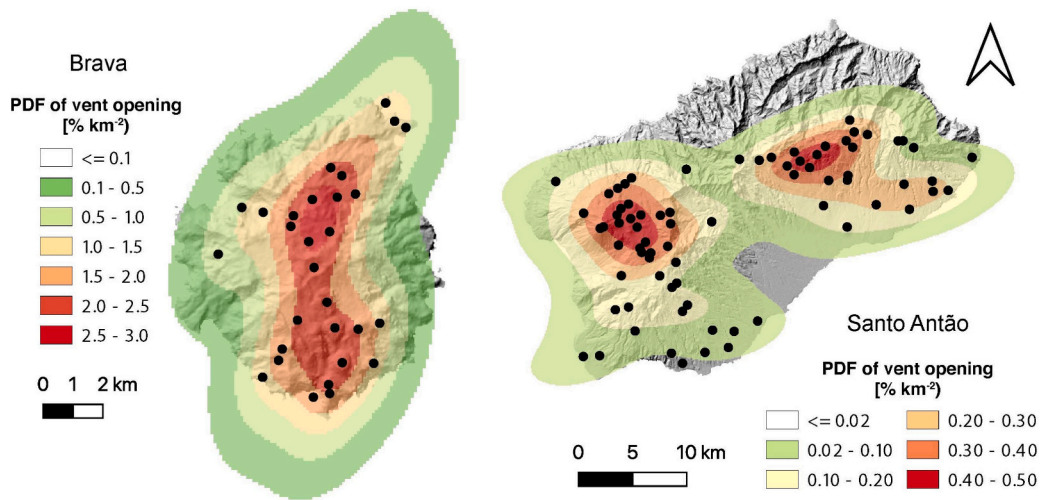
Fig. 11. Model for spatial density (% per km²) of volcanic vents on a) Brava island, based on 29 identified vents, and b) Santo Antão island, based on 76 identified vents. Note that spatial density is higher on Brava. While the uncoloured areas have a very low modelled density, density does not decrease to zero for any point on the islands.
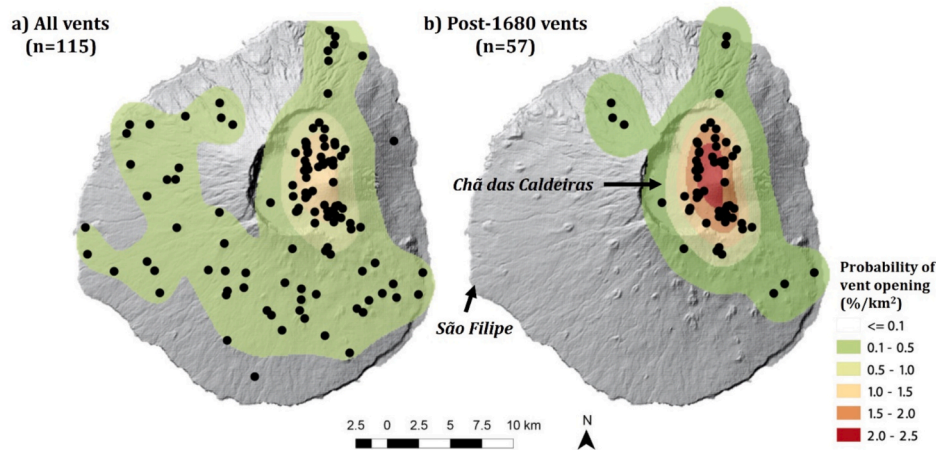
Fig. 12. Model for spatial density of volcanic vents on Fogo island, based on all 115 (left) and only the 57 post-1680 (right) identified vents.

not a single calculated value from a future event, high impact scenarios that might lead to unacceptable consequences (e.g. [39]) may not be well represented. For example, the city of Addis Ababa lies 130 km downwind from Fentale: a distance easily travelled by tephra in a future eruption but one that does not lie within the return period footprints presented here. Similarly, the city of Nairobi lies upwind (east) from prevailing easterly winds at Suswa; however, during October and November, winds can blow directly from Suswa and disperse tephra to Nairobi.

While the drainage basin analysis does not forecast flow paths, it does use topography to highlight areas susceptible to flows. For Ethiopia and Kenya, such areas are constrained by the presence of sharp topographic changes due to the presence of rift-parallel fault scarps, horsts, and grabens generally orientated N-S to NE-SW, as well as by numerous lakes that act as sinks for flowing material. This was particularly evident at Aluto in Ethiopia, which had the smallest identified flow hazard area (117 km²; Fig. 8); however, visual inspection shows that should the topographic barrier towards the west be overcome, it is clear that the impacted area would be much larger and include the flat area west-southwest of the volcano. By contrast, the larger footprint of Longonot in Kenya (1102 km²) occurred because the volcanic topography comprised one central volcano and a relatively flat surrounding landscape until the bordering rift scarps ~30 km to the east and west (Fig. 8).

The sensitivity of our results to GVP vent locations, which may not represent the site of a future eruption, was significant for those volcanoes and volcanic complexes with more complex topography. For example, when assuming the centre of the summit crater as the vent location for Suswa, the potential hazard zone extends almost 30 km to the north of the volcano, an area that is apparently untouched when assuming the highest point of the volcano (crater rim) as vent location (Fig. 9).

Vent spatial density maps for the islands of Cabo Verde, where flank vents are prevalent, showed bimodal areas of elevated vent opening probabilities on Santo Antão, related to the two main volcanoes, and broad north-south elongations of high probabilities on Brava and Fogo (Fig. 11 and Fig. 12), likely related to stress fields within the volcano edifice [31,40,41]. The Fogo spatial density maps of Richter et al. [42], who considered 42 vents within Chã das Caldeiras, showed a similar trend, albeit with slightly higher probabilities due to their omission of vents outside of Chã das Caldeiras. The influence of vent age on forecasting vent opening in Fogo was to focus areas of higher probability, when a shorter timeframe was considered; this reflects spatial and temporal clustering in the record. Detailed dating work is needed to determine spatial changes in vent opening over time (e.g. [43]). Where vent age data are available, using only vents from the most recent 'cluster' of activity is going to be more indicative of the next vent
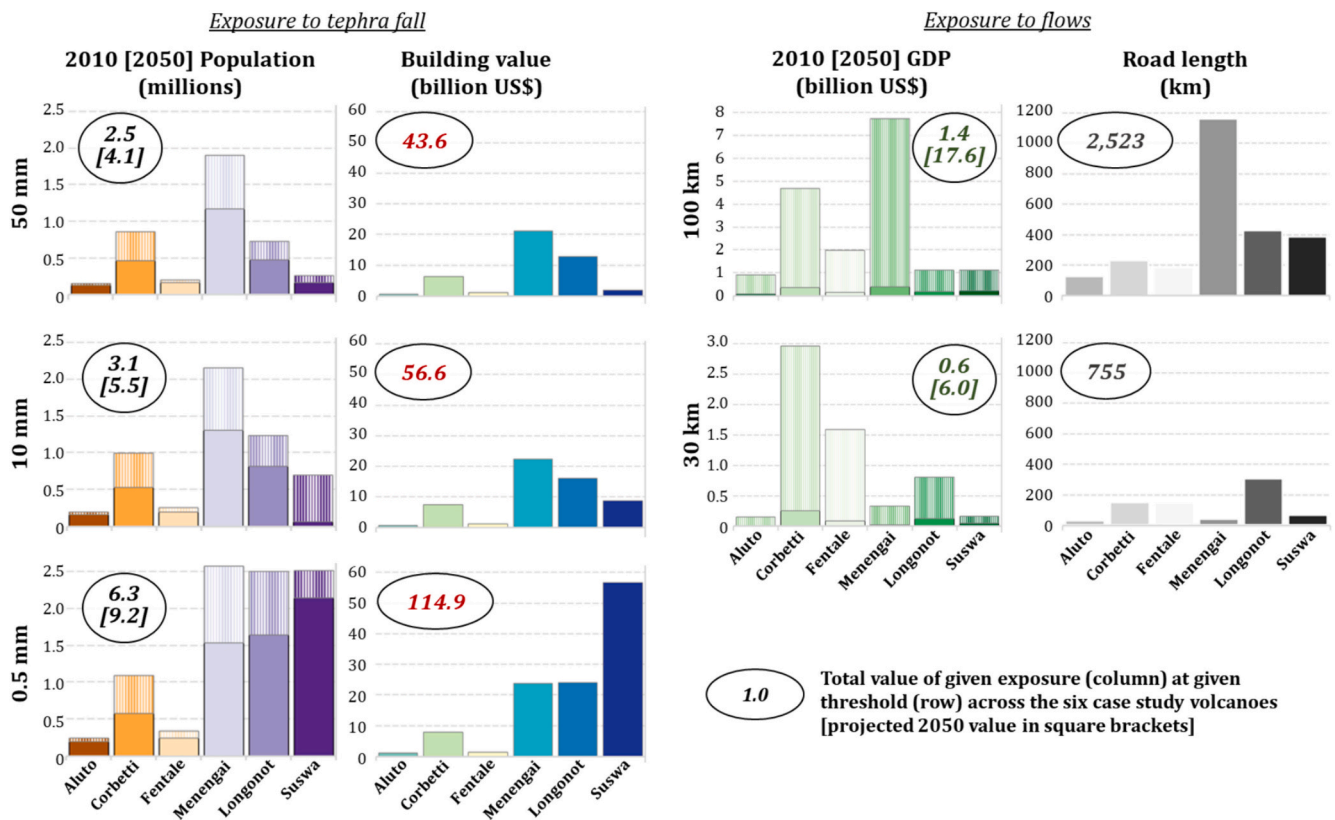
Fig. 13. Selected exposure estimates for the six target volcanoes of Ethiopia and Kenya (the island volcanoes of Cabo Verde produce smaller exposure and are not shown here). All exposure data are available in Supplementary Material G. The four columns of charts represent different exposed assets and the rows the different tephra thickness thresholds at the 1000-year return period (left two columns) and drainage basins within set buffers from the vent (right two columns). For population (1st column) and GDP (3rd column) projected values for 2050 are also shown by the lined overlay bars. The total exposure value across the six volcanoes is shown for each chart by the circled value [projected 2050 values in square brackets where applicable]. 1 million is 1×10^6, 1 billion is 1×10^9.

Table 2

Comparison of calculated populations within a) 10 km, b) 30 km, and c) 100 km radius of the target volcanoes in Ethiopia and Kenya. Bubble areas represent the populations within each radius. Population datasets are WorldPop [32], Land-Scan [33], and Gridded Population of the World (GPW v4: [34]): all datasets were globally available, open-access, from the same year (2015) and with the same spatial resolution (~1 km²). WorldPop was used for population exposure calculations in the rest of this study.

Volcano	Radii (km)	WorldPop	LandScan	GPW
Corbetti	10	59,527	42,425	114,726
	30	1,188,562	1,171,948	1,599,303
	100	12,832,586	9,794,061	13,224,700
Aluto	10	30,457	25,619	46,602
	30	357,905	314,216	484,976
	100	8,965,106	6,813,710	8,997,593
Fentale	10	26,100	14,201	26,945
	30	171,206	169,357	208,905
	100	4,504,967	3,482,286	4,284,752
Menengai	10	250,531	204,608	187,356
	30	992,625	886,293	1,058,221
	100	5,362,753	4,259,089	5,237,656
Longonot	10	18,101	17,893	28,718
	30	449,298	410,677	523,305
	100	11,514,963	8,750,154	10,758,323
Suswa	10	2393	4041	7293
	30	111,623	105,232	183,261
	100	9,688,232	6,914,644	9,356,564

location, while incorporating more vents from a longer time frame will provide a longer-term view of spatio-temporal trends in likely vent opening locations.

While cities concentrate areas of high exposure, important infrastructure can be present in areas of otherwise low exposure. For example, major roads pass very close to our target volcanoes, with the main road from Kenya (Nairobi) to Uganda within 13 km of Longonot and Menengai, the main road from Djibouti into Ethiopia within 8 km of Fentale summit and the main route from Ethiopia into Nairobi within 13 km of Aluto and Corbetti. Evaluating the criticality, capacity, demand, and surface material of roads would be an important addition to assessing road length (e.g. [44,45]). Geothermal power plants are operational near the GVP-defined Aluto crater (~2.5 km), and investigations are underway for new plant sites near Fentale and Corbetti volcanoes. These can provide power for people, industry, and activities at distances far beyond those reached by volcanic hazards, meaning any disruption to service can affect a much greater number of people.

Our findings on sensitivity to population data support the findings of Vye-Brown et al. [46] who carried out a similar exposure comparison exercise for Ethiopian volcanoes. For relative comparisons of exposure across volcanoes, the population data source appears to be less important; however, for absolute calculations of populations exposed, or for local-scale (community) calculations of exposure, for example for emergency management planning, local data sources such as recent government census/population mapping will be more appropriate.

4.1. Ways forward

The regional assessment presented here was used to highlight volcanic threat at the inter-governmental organisation and policy-maker level, and forms part of a process to develop the knowledge and evidence base for volcanic risk reduction. A key challenge throughout our study was the lack of data and knowledge surrounding our target volcanoes and their eruptive history, which we tackled through expert

elicitation and the development of new data, where possible (e.g. vent mapping from satellite imagery). Although the study was instrumental in supporting subsequent joint research initiatives (e.g. Riftvolc), more is needed. We see seven key areas for improvement, to better support our ability to carry out volcanic hazard and risk assessments in the region:

1. Investment in long-term joint research initiatives including scientists in two or more countries to support and foster long-standing collaboration, partnerships and knowledge exchange, with essential inclusion and funding of in-country scientists. Their local data, knowledge, context and relationships with decision makers and communities are imperative to the development of robust assessments. Resources for such studies may come from local or national government but also international organisations such as the Africa Disaster Risk Financing Initiative.

2. National to regional scale understanding of volcanoes and the threat they pose to highlight priorities and needs, and to provide an evidence base for the targetting of resources, e.g. NVEWS: Ewert et al. 2007.

3. Volcano monitoring capability needs to be enhanced so that recognised high risk volcanoes, especially those demonstrating unrest (see (3) below), are monitored by a combination of complementary multi-parameter techniques (see recommendations in [2]). Donations of equipment and knowledge transfer schemes must be practical in the short-term (planned and designed with in-country scientists) and sustainable in the long term. Support for developing and sustaining local/national infrastructure and expertise is essential. Volcanoes are unlike many natural hazards because if a volcano is monitored and there are appropriate institutional systems and protocols in place, then it is possible to accurately forecast eruptions and volcanic hazards so that mitigating actions can be taken and losses reduced.

4. More geological and geochronological studies to address critical knowledge gaps. These will help to build a more complete eruption database for the East African Rift and Cabo Verde, which will refine eruption frequency-magnitude relationships and their uncertainty (essential to understand hazard and risk). We recommend that detailed mapping and dating of volcanic products be made a priority for the six volcanoes that were identified as targets in this study, perhaps with an immediate focus on those showing signs of unrest, e. g. seismic swarms in Brava in 2016 [47] and 2023 and repeatedly on Santo Antão; sustained uplift at Corbetti for more than a decade [3]; and the 2015 seismic swarm at Fentale [48].

5. Collection of quantitative data regarding eruption deposit characteristics such as lava flow and pyroclastic density current volumes, tephra fall extent, thickness and grainsizes, and other hazard-specific data and analysis to inform future hazard estimates. This includes structural and spatio-temporal analysis of vent distribution to support understanding of likely future vent opening. Both past and future eruptions, and their impacts, need characterising to understand hazard and risk.

6. In the absence of intensive and/or long-term research initiatives, similar elicitation exercises carried out in-country with more local experts than could join this study would help in further identifying data and knowledge gaps, and our uncertainties. For example, further discussion around the potential over-assignation of VEI 4 eruptions in the historical record, and the likely preservation of deposits in the region would be valuable, as well as whether gaps in the geological record are real or not.

7. Moving volcanic hazard and exposure assessments towards risk requires improved knowledge of volcanic impacts, which is constrained to anecdotal evidence and a relatively small number of post-eruption impact assessments [49]. The physical vulnerability of buildings and infrastructure could be inferred from recent eruptions in the region (e.g. [50]; Michelier et al., 2020), and/or analogous exposures worldwide, using established guidelines that are available for assessing physical vulnerability to volcanic hazards (e.g. [51]).

8. Finally, volcanic risk must be considered in the context of other natural (and non-natural) hazards that threaten the exposed communities. Building on the multi-hazard disaster risk profiles developed as part of this project, more detailed evaluation of both volcanic and other hazards together may be useful to better understand the threat posed.

5. Conclusions

We outline our approach to assessing volcanic hazard and exposure for data-poor volcanoes in Ethiopia, Kenya and Cabo Verde, as part of a larger multi-hazard risk profiling effort for sub-Saharan Africa. To keep the project focussed and tractable, and because of a lack of data, we restricted our analysis to nine target volcanoes suggested by in-country scientists and did not consider the vulnerability of exposed assets. All target volcanoes were characterised by poor data regarding their eruptive history and, as past activity is the best indicator of likely future activity at a volcano, this posed a problem for hazard assessment. To identify areas of hazard around the selected target volcanoes we elicited experts to derive frequency-magnitude relationships and ESPs for each volcano, mapped past eruptive centres, and coupled this with numerical modelling of tephra dispersion, vent opening, and GIS analysis of drainage basins around each volcano. Volcano-specific hazard footprints that fully account for variability in wind conditions, vent locations and eruption characteristics were thus created and aggregated as a function of repose interval, before being coupled with exposure data on population, infrastructure and transport. This provided the first such hazard and exposure assessments for these volcanoes.

Fogo volcano, Cabo Verde, was considered the most frequently erupting volcano from our elicited volcanoes, and Aluto and Corbetti, Ethiopia, the least, with an eruption of any VEI expected on average every 20 and 308 years, respectively (Table 1). Fentale (Ethiopia), Longonot and Suswa (Kenya) were elicited to have the greatest probability for a moderate to large explosive (VEI ≥ 4) eruption (on average every 400 years), based on the known geology and similarities to the better studied Rungwe volcano in Tanzania. Discussions as part of the elicitation suggested that emergency management should plan for extended eruption durations of months to years. The strong seasonal influence on tephra dispersion means that areas to the north and south of the volcanoes are less affected than those to the east and west. Although not considered in this analysis, gas emissions would be similarly controlled by wind direction. Menengai and Longonot produce the larger exposure values across most VEI scenarios and categories of exposure, but for more distal tephra fall and flow exposures, Corbetti and Suswa also exhibit high exposures. Potentially high impact scenarios that warrant more in-depth investigation include tephra being dispersed across large cities (e.g. Nairobi, 55 km from Suswa) and key infrastructure, such as roads and geothermal power stations (e.g. ~2.5 km from Aluto), as well as important tourist destinations, seats of government and emergency management operations (e.g. islands east of Fogo).

The areas identified as susceptible to flows were strongly influenced by the assumed vent location and, to a lesser extent, by the resolution of the underlying DEM. This was particularly the case for volcanoes with more complex topography. We suggest that a DEM resolution of 90 m is ideal for these more simplistic drainage basin analyses so that topography does not over- or under-control the results. The small size of the volcanic islands of Cabo Verde placed much of the islands at risk from future flows, especially on Brava, which has had recent unrest and has no strong topographic features; this has important implications for the safe and timely evacuation of people during a future explosive eruption. For volcanoes with prominent topography, the drainage basin analyses were strongly influenced by the location of the vent. Vent mapping on the volcanic islands of Cabo Verde showed that future vents are most likely to open on broad north-south elongations across Fogo and Brava, and around the two main volcanoes of Santo Antão.

The study provided new data, hazard and exposure analyses, and a framework for carrying out a volcanic hazard and exposure assessment where few data on past eruptions are available. This work highlights the importance of volcanic risk within multi-hazard assessments at the regional to global level and provides the background for more detailed hazard and risk studies in the region. We draw attention to seven key areas where data gathering would benefit volcanic hazard and risk assessment: key to these is investment in monitoring and geological and geochemical studies so that eruption, hazard, and impact forecasts could be more robustly made. This work contributes to Goal 11 (make cities and human settlements inclusive, safe, resilient and sustainable) of the Sustainable Development Goals ([52]–2030). and the Sendai Framework for Disaster Risk Reduction 2015–2030. In particular, better understanding of hazards and potential impacts is the first step towards mitigation and management of future disasters. Further collaborative efforts following the recommendations arising from this study, including scientists, decision makers and communities, will contribute to reduce the number of disaster-related deaths, directly affected people, direct economic loss in relation to GDP and damage to critical infrastructure in future disasters.

CRediT authorship contribution statement

S.F. Jenkins: Conceptualization, Data curation, Formal analysis, Funding acquisition, Methodology, Visualization, Writing – original draft, Writing – review & editing. **K. Mee:** Conceptualization, Data curation, Formal analysis, Methodology, Visualization, Writing – review & editing. **S.L. Engwell:** Conceptualization, Data curation, Formal analysis, Visualization, Methodology, Writing – review & editing. **S.C. Loughlin:** Conceptualization, Funding acquisition, Methodology, Project administration, Writing – review & editing. **B.V.E. Faria:** Methodology, Validation, Writing – review & editing. **G. Yirgu:** Methodology, Validation, Writing – review & editing. **Y. Bekele:** Methodology, Validation, Writing – review & editing. **E. Lewi:** Methodology, Validation, Writing – review & editing. **C. Vye-Brown:** Methodology, Validation, Writing – review & editing. **S.A. Fraser:** Conceptualization, Methodology, Validation, Writing – review & editing. **S.J. Day:** Methodology, Validation, Writing – review & editing. **R.M. Lark:** Conceptualization, Data curation, Formal analysis, Methodology, Writing – review & editing. **C. Huyck:** Validation, Writing – review & editing, Data curation. **J. Crummy:** Validation, Writing – review & editing.

Declaration of competing interest

The authors declare that they have no known competing financial interests or personal relationships that could have appeared to influence the work reported in this paper.

Data availability

Research data presented in this study are available at the NTU Data Repository: https://researchdata.ntu.edu.sg/privateurl.xhtml?token=02556fe6-88ca-46e8-9342-1f94977594c2

(a private url is provided during the review process, but the data will be published publicly when the associated paper is published)

Acknowledgements

Appendix A. Supplementary data

Supplementary data to this article can be found online at https://doi.org/10.1016/j.pdisas.2024.100350.

References

[1] Ward PJ, Blauhut V, Bloemendaal N, Daniell JE, de Ruiter MC, Duncan MJ, et al. Natural hazard risk assessments at the global scale. Nat Hazards Earth Syst Sci 2020;20.
[2] Loughlin SC, Sparks RSJ, Brown SK, Jenkins SF, Vye-Brown C. Global volcanic hazards and risk. Cambridge University Press; 2015.
[3] Biggs J, Ayele A, Fischer TP, Fontijn K, Hutchison W, Kazimoto E, et al. Volcanic activity and hazard in the East African Rift Zone. Nat Commun 2021;12(1):6881.
[4] Keir D, Bastow ID, Corti G, Mazzarini F, Rooney TO. The origin of along-rift variations in faulting and magmatism in the Ethiopian Rift. Tectonics 2015;34(3):464–77.
[5] Yirgu G, Ebinger CJ, Maguire PKH. The afar volcanic province within the East African Rift System: introduction. Geol Soc Lond Spec Publ 2006;259(1):1–6.
[6] Ramalho RS, Helffrich G, Cosca M, Vance D, Hoffmann D, Schmidt DN. Vertical movements of ocean island volcanoes: insights from a stationary plate environment. Mar Geol 2010;275:84–95. https://doi.org/10.1016/j.margeo.2010.04.009.
[7] Brown SK, Auker MR, Sparks RSJ. Populations around Holocene volcanoes and development of a Population Exposure Index. Global Volcanic Hazards Risk 2015:223–32.
[8] Clarke B, Tierz P, Calder E, Yirgu G. probabilistic volcanic hazard assessment for pyroclastic density currents from pumice cone eruptions at Aluto volcano, Ethiopia. Front Earth Sci 2020;8.
[9] Colby DJ, Pyle DM, Fontijn K, Mather TA, Melaku AA, Mengesha MA, et al. Stratigraphy and eruptive history of Corbetti Caldera in the Main Ethiopian Rift. J Volcanol Geotherm Res 2022;428:107580.
[10] Hutchison W, Pyle DM, Mather TA, Yirgu G, Biggs J, Cohen BE, et al. The eruptive history and magmatic evolution of Aluto volcano: new insights into silicic peralkaline volcanism in the Ethiopian rift. J Volcanol Geotherm Res 2016;328:9–33.
[11] Tadesse A, Fontijn K, Melaku A, Gebru E, Smith V, Tomlinson E, et al. Eruption frequency and magnitude in a geothermally active continental rift: the Bora-Baricha-Tullu Moye volcanic complex, Main Ethiopian Rift. J Volcanol Geotherm Res 2022;423:107471.
[12] Tierz P, Clarke B, Calder ES, Dessalegn F, Lewi E, Yirgu G, et al. Event trees and epistemic uncertainty in long-term volcanic hazard assessment of rift volcanoes: the example of Aluto (Central Ethiopia). Geochem Geophys Geosyst 2020;21:e2020GC009219.
[13] McNamara K, Cashman K, Rust A, Fontijn K, Chalié F, Tomlinson EL, et al. Using lake sediment cores to improve records of volcanism at Aluto volcano in the Main Ethiopian Rift. Geochem Geophys Geosyst 2018;19:3164–88.
[14] Fontijn K, McNamara K, Tadesse AZ, Pyle DM, Dessalegn F, Hutchison W, et al. Contrasting styles of post-caldera volcanism along the Main Ethiopian rift: implications for contemporary volcanic hazards. J Volcanol Geotherm Res 2018;356:90–113.
[15] Martin-Jones CM, Lane CS, Pearce NJ, Smith VC, Lamb HF, Schaebitz F, et al. Recurrent explosive eruptions from a high-risk Main Ethiopian Rift volcano throughout the Holocene. Geology 2017;45:1127–30.
[16] Siegburg M, Gernon TM, Bull JM, Keir D, Barfod DN, Taylor RN, et al. Geological evolution of the Boset-Bericha volcanic complex, Main Ethiopian Rift: 40Ar/39Ar evidence for episodic Pleistocene to Holocene volcanism. J Volcanol Geotherm Res 2018;351:115–33.
[17] Cooke R, Mendel M, Thijs W. Calibration and information in expert resolution. Class Apprch Automatica 1988;24(1):87–93.
[18] Gosling JP. SHELF: The Sheffield elicitation framework. In: Elicitation. Springer; 2018. p. 61–93.
[19] Bonadonna C, Connor CB, Houghton BF, Connor L, Byrne M, Laing A, et al. probabilistic modeling of tephra dispersal: Hazard assessment of a multiphase rhyolitic eruption at Tarawera, New Zealand. J Geophys Res 2005;110:1–21.
[20] Jenkins S, Magill C, McAneney J, Blong R. Regional ash fall hazard I: a probabilistic assessment methodology. Bull Volcanol 2012;74:1699–712. https://doi.org/10.1007/s00445-012-0627-8.

[21] Aspinall WP, Auker MR, Hincks TK, Mahony SH, Pooley J, Nadim F, et al. Volcano hazard and exposure in track II countries and risk mitigation measures - GFDRR volcano risk study, 309. 2011.

[22] Connor LJ, Connor CB, Meliksetian K, Savov I. Probabilistic approach to modeling lava flow inundation: a lava flow hazard assessment for a nuclear facility in Armenia. J Appl Volcanol 2012;1:1–19. https://doi.org/10.1186/2191-5040-1-3.

[23] Jenkins SF, Wilson TM, Magill CR, Miller V, Stewart C, Blong R, et al. In: Loughlin SC, Sparks RSJ, Brown SK, Jenkins SF, Vye-Brown C, editors. Volcanic ash fall hazard and risk. Chapter 3, in: Global Volcanic Hazards and Risk. 173. Cambridge, UK: Cambridge University Press; 2015. Open Access: cambridge.org/volcano.

[24] Hayes JL, Wilson TM, Magill C. Tephra fall clean-up in urban environments. J Volcanol Geotherm Res 2015;304:359–77.

[25] Jenkins SF, Magill CR, Blong RJ. Evaluating relative tephra fall hazard and risk in the Asia-Pacific region. Geosphere 2018;14:492–509.

[26] Jenkins SF, Biass S, Williams GT, Hayes JL, Tennant E, Yang Q, et al. Evaluating and ranking Southeast Asia's exposure to explosive volcanic hazards. Nat Hazards Earth Syst Sci 2022:1233–65.

[27] Wiart P, Oppenheimer C. Largest known historical eruption in Africa: Dubbi volcano, Eritrea, 1861. Geology 2000;28:291–4.

[28] Goitom B, Oppenheimer C, Hammond J, Grandin R, Barnie T, Donovan A, et al. First recorded eruption of Nabro volcano, Eritrea, 2011. Bull Volcanol 2015;77-85.

[29] Mastin L, Guffanti M, Servranckx R, Webley P, Barsotti S, Dean K, et al. A multidisciplinary effort to assign realistic source parameters to models of volcanic ash-cloud transport and dispersion during eruptions. J Volcanol Geotherm Res 2009;186:10–21.

[30] Scollo S, Tarantola S, Bonadonna C, Coltelli M, Saltelli A. Sensitivity analysis and uncertainty estimation for tephra dispersal models. J Geophys Res-Solid Earth Artn 2008;113:B06202. https://doi.org/10.1029/2006jb004864.

[31] Day SJ, Heleno da Silva SIN, Fonseca JFBD. A past giant lateral collapse and present-day flank instability of Fogo, Cape Verde Islands. J Volcanol Geotherm Res 1999;94:191–218. https://doi.org/10.1016/S0377-0273(99)00103-1.

[32] Tatem AJ. WorldPop, open data for spatial demography. Sci data 2017;4(1):1–4.

[33] Bright E, Rose A, Urban M. LandScan global 2015. LandScan Global; 2016.

[34] CIESN, Center for International Earth Science Information Network - Columbia University. 2016. Gridded Population of the World, Version 4 (GPWv4): Population Density. Palisades, NY: NASA Socioeconomic Data and Applications Center (SEDAC). https://doi.org/10.7927/H4NP22DQ. Accessed 12 October 2019.

[35] Martin-Jones CM, Lane CS, Pearce NJG, Smith VC, Lamb HF, Schaebitz F, et al. Recurrent explosive eruptions from a high-risk Main Ethiopian Rift volcano throughout the Holocene. Geology 2017;45:1127–30. https://doi.org/10.1130/g39594.1.

[36] Eisele S, Reißig S, Freundt A, Kutterolf S, Nürnberg D, Wang K, et al. Pleistocene to Holocene offshore tephrostratigraphy of highly explosive eruptions from the southwestern Cape Verde Archipelago. Mar Geol 2015;369:233–50.

[37] Burgos V, Jenkins SF, Bono Troncoso L, Perales Moya CV, Bebbington M, Newhall C, et al. Identifying analogues for data-limited volcanoes using hierarchical clustering and expert knowledge: a case study of Melimoyu (Chile). Front Earth Sci 2023;11:1144386.

[38] Hayes JL, Jenkins SF, Joffrain M. Large uncertainties are pervasive in long-term frequency-magnitude relationships for volcanoes in Southeast Asia. Front Earth Sci 2022;10:895756.

[39] Lin Y, Jenkins S, Chow J, Biass S, Woo G, Lallemant D. Modeling downward counterfactual events: unrealized disasters and why they matter. Front Earth Sci 2020;8:575048.

[40] Faria BV, Day S, Fonseca JF. Insights from geophysical monitoring into the volcano structure and magma supply systems at three very different oceanic islands in the Cape Verde archipelago. In: AGU fall meeting abstracts. 2013; 2013. V41B-2786.

[41] Faria B, Fonseca JFBD. Investigating volcanic hazard in Cape Verde Islands through geophysical monitoring: network description and first results. Nat Hazards Earth Syst Sci 2014;14(2):485–99.

[42] Richter N, Favalli M, de Zeeuw-van Dalfsen E, Fornaciai A, Fernandes R, Perez Rodriguez N, et al. Lava flow hazard at Fogo volcano, Cape Verde, before and after the 2014-2015 eruption. Nat Hazards Earth Syst Sci Dis 2016. https://doi.org/10.5194/nhess-2016-81, 2016.

[43] Foeken JP, Day S, Stuart FM. Cosmogenic 3He exposure dating of the Quaternary basalts from Fogo, Cape Verdes: implications for rift zone and magmatic reorganisation. Quat Geochronol 2009;4(1):37–49.

[44] Blake DM, Wilson TM, Cole JW, Deligne NI, Lindsay JM. Impact of volcanic ash on road and airfield surface skid resistance. Sustainability 2017;9:1389.

[45] Hayes JL, Biass S, Jenkins SF, Meredith ES, Williams GT. Integrating criticality concepts into road network disruption assessments for volcanic eruptions. J Appl Volcanol 2022;11:1–21.

[46] Vye-Brown C, Sparks RSJ, Lewi E, Mewa G, Asrat A, Loughlin SC, et al. Ethiopian volcanic hazards: a changing research landscape. Geol Soc Lond Spec Publ 2016; 420(1):355–65.

[47] Leva C, Rümpker G, Wölbern I. Remote monitoring of seismic swarms and the August 2016 seismic crisis of Brava, Cabo Verde, using array methods. Nat Hazards Earth Syst Sci 2020;20(12):3627–38.

[48] Whaler K, Atalay A, Luckett R, Baptie B. The 2015 earthquake swarm in the Fentale volcanic complex (FVC): a geohazard risk for Ethiopia's commercial route to the Djibouti port. J African Earth Sci 2024;213(105236).

[49] Deligne NI, Jenkins SF, Meredith ES, Williams GT, Leonard GS, Stewart C, et al. From anecdotes to quantification: advances in characterizing volcanic eruption impacts on the built environment. Bull Volcanol 2022;84:1–9.

[50] Wantim MN, Bonadonna C, Gregg CE, Menoni S, Frischknecht C, Kervyn M, et al. Forensic assessment of the 1999 Mount Cameroon eruption, West-Central Africa. J Volcanol Geotherm Res 2018;358:13–30.

[51] Jenkins SF, Spence RJS, Fonseca JFBD, Solidum RU, Wilson TM. Volcanic risk assessment: quantifying physical vulnerability in the built environment. J Volcanol Geotherm Res 2014;276:105–20. https://doi.org/10.1016/j.jvolgeores.2014.03.002.

[52] UNISDR (United Nations International Strategy for Disaster Reduction): Sendai framework for disaster risk reduction 2015–2030. Geneva: https://www.preventionweb.net/sendai-framework/sendai-framework-for-disaster-risk-reduction; 2015 (accessed 7 March 2023).